CELLULOSE CHEMISTRY AND TECHNOLOGY

INVESTIGATION OF CARBOXYMETHYL CELLULOSE INCORPORATION EFFECTS ON TFC MEMBRANE ACTIVE LAYERS USING VARIOUS SUPPORTS

HANANE ABURIDEH, DJAMILA ZIOUI, SARRA HOUT, ZOUBIR BELGROUN,
FATMA ZOHRA YAHIAOUI and MOHAMED ABBAS

Unité de Développement des Equipements Solaires, UDES/Centre de Développement des Energies Renouvelables, CDER, Bou Ismail, 42415, W. Tipaza, Algeria
✉ *Corresponding author: H. Aburideh, h_aburideh@yahoo.fr*

Received July 22, 2024

Thin film composite (TFC) membranes have been widely used in saline water treatment. However, challenges remain in their development, particularly regarding the trade-off between permeability and selectivity. This work focuses on fabricating TFC nanofiltration (NF) membranes coated with a carboxymethyl cellulose sodium (CMC-Na) solution to address this compromise. TFC membranes are developed in several steps, starting with the formation of a support polymer layer through the non-solvent induced phase separation (NIPS) process. Interfacial polymerization (PI) was successfully performed on cellulose acetate (AC), polyacrylonitrile (PAN), and polyethersulfone (PES) supports. An active layer of polyamide (PA) was obtained by the condensation reaction between piperazine (PIP) and trimesoyl chloride (TMC). The permeability and selectivity of the TFC membranes were evaluated by incorporating the CMC solution. The membranes were characterized based on their flux, hydraulic permeability, and selective permeability. The physicochemical properties of the manufactured membranes were analyzed using FTIR, water content measurements, and material transfer assessments. The TFC PAN B3 membrane exhibited the best flux and permeability, achieving values of 500 L/m².h and 24 L/m².h.bar, respectively. In contrast, the TFC PES C3 membrane demonstrated superior efficiency in rejecting Mg^{2+}, Ca^{2+}, and NaCl, with respective rejection rates of 66%, 60%, and 67%.

Keywords: TFC thin film composite membrane, cellulose acetate, polyacrylonitrile, polyethersulfone, sodium carboxymethyl cellulose (CMC-Na), PI interfacial polymerization

INTRODUCTION

Water availability remains a significant problem for the 45 million people in our country affected by severe water stress. The use of polymers has enabled the development of composite membranes for large-scale seawater desalination at a cost ten times lower than traditional distillation technology.[1-3] The application of membrane processes in industry has effectively reduced energy costs and the environmental impact of production waste. After revolutionizing hemodialysis and improving the daily lives of millions of patients with kidney failure, polymer filtration membranes have become the benchmark technology for water filtration and drinking water production. From individual portable treatment systems to production plants exceeding 150,000 m³/day, polymer membranes consistently provide pure and high-quality water.[4] Due to their diverse properties, polymers have facilitated the development of membrane processes for disinfection, water softening, and desalination.

Membrane purification processes have quickly become the preferred technology for water treatment, primarily due to their operational simplicity and lower energy consumption compared to conventional methods. Nanofiltration and reverse osmosis (RO) membranes are used to remove dissolved solutes, such as salts and organic and inorganic matter from water.[5] These membranes have smaller pore sizes and employ a combination of size exclusion and charge repulsion as separation mechanisms. Research and practical applications in this field dominated until the early 1980s, when John Cadotte invented the polyamide thin-film composite (PA-TFC) membrane through interfacial polymerization. This membrane is produced by the reaction of piperazine in an aqueous solution with a trimesoyl chloride derivative in an organic solvent. These membranes have demonstrated great potential in saltwater treatment due to their excellent performance and versatility.[6-8] Subsequent years saw trials aimed at enhancing the overall performance and physicochemical properties of these membranes. Although some challenges remain, they continue to be unmatched in terms of low cost, acceptable performance, straightforward synthesis and scale-up possibilities. Numerous attempts have been made to develop different types of membranes through simulation and practical manufacturing, employing various materials and techniques.[9]

The main advantage of composite membranes is that each layer can be optimized separately to achieve the desired separation performance. Generally, mixing different polymers is an inexpensive and effective method for obtaining new structural materials.[10] Cellulose and its derivatives, being biopolymers derived from abundant and sustainable sources, represent a well-known family of membranes.[11-13]

Cellulose is a promising material for applications in membrane technology, offering ecological advantages and efficiency in various industrial processes. Its numerous hydroxyl groups facilitate the preparation of membranes and hydrogels with unique structures and properties. Cellulose derivatives, such as methylcellulose (MC), hydroxypropylcellulose (HPC), hydroxypropylmethylcellulose (HPMC), and carboxymethylcellulose (CMC), have been utilized to fabricate cellulose-based hydrogels through physical and chemical crosslinking. These derivatives are considered promising solutions for water treatment challenges, combining technological innovation with environmental sustainability.

Carboxymethylcellulose based hydrogels provide numerous advantages in water treatment, contributing to purification, pollutant absorption, and enhanced efficiency of treatment systems. Their unique properties and the ability to modify them make them valuable tools for specific applications in water resource management. Typically, they are manufactured using methods such as freeze-drying, radical polymerization, or chemical cross-linking, the latter of which enhances the mechanical strength and stability of the membranes.[14-15]

This work targets several objectives. The first is to develop new TFC membranes by introducing an additional layer of a hydrophilic compound, such as sodium carboxymethyl cellulose (CMC-Na), to improve performance in terms of flux and permeability. The second objective involves using different types of polymeric materials for the fabrication of the lower layer of the TFC membrane to compare their effects on membrane morphology and efficiency. The final objective is to validate the performance of the membranes regarding flux and rejection rates while maintaining optimal flux and improving membrane selectivity.

EXPERIMENTAL

Materials

Polyethersulfone (PES, chemical name: poly(oxy-1,4-phenylenesulfonyl-1,4-phenylene)), cellulose acetate (AC, M = 50,000 g/mol), and polyacrylonitrile (PAN, M = 150,000 g/mol) were supplied by Sigma Aldrich, and used for fabricating the membrane support. Carboxymethyl cellulose sodium (CMC-Na, degree of substitution = 0.7, average molecular weight = 250,000) is a cellulose derivative acquired from Aldrich and was employed as a hydrophilic agent. Polyethylene glycol (PEG, M = 2000) was obtained from Biochem and used as a porogenic compound. Piperazine (PIP, M = 108.14 g/mol), sourced from Biochem, was utilized as a diamine substrate for preparing the inorganic part. Trimesoyl chloride (TMC, M = 108.14 g/mol) was provided by VWR Chemicals and selected as the chlorinated derivative for conducting interfacial polymerization. Other products used during filtration tests and analytical techniques included salts, such as sodium chloride (NaCl), calcium carbonate ($CaCO_3$), obtained from Biochem Lab, and magnesium sulfate ($MgSO_4$), purchased from Sigma Aldrich.

Membranes manufacturing

Method for producing membrane supports

Three types of ultrafiltration (UF) membranes were fabricated using PES, PAN and CA as polymers. These membranes were prepared by the phase inversion method, specifically through Non-Solvent Induced Phase Separation (NIPS), as illustrated in Figure 1. The resulting films served as supports for the fabrication of TFC membranes.

PES membranes were prepared by dissolving 18% by weight of polyethersulfone in N,N-dimethylformamide (DMF) with constant stirring at 300 rpm for 24 hours at 60 °C. A homogeneous solution was obtained and allowed to rest without stirring for 30 minutes to eliminate air bubbles. Similarly, 13% PAN and 18% CA were dissolved in 80% DMF and N-methyl-2-pyrrolidone (NMP), respectively, under the same stirring conditions for 12 hours at 60 °C.[16-17]

After obtaining a homogeneous solution, it was also left to rest for 30 minutes to remove air bubbles. The collodions were then spread on a glass plate using a casting knife and immersed in a coagulation bath. During this process, the polymer film underwent progressive transformation from a liquid phase (transparent) to a solid phase (whitish), gradually detaching from the glass plate. The membrane film was subsequently transferred to a bath of demineralized water for 24 hours to facilitate the exchange between solvent and non-solvent.

Preparation of thin film composite (TFC) membranes

The formation of a cross-linked polyamide layer on the membrane was achieved through interfacial polymerization between PIP and TMC on AC, PES, or PAN supports, as illustrated in Figure 2. The procedure is as follows:

1. After removing excess water, an aqueous solution containing 2% by weight of PIP was poured onto the substrate and left in contact for 10 minutes;
2. The membrane surface was carefully wiped with a paper towel and a rubber roller to remove any excess PIP;
3. A solution of n-hexane containing 0.7% by weight of TMC was poured onto the membrane surface and allowed to react for a specified period;
4. The obtained membranes were quickly air-dried and then placed in an oven for 15 minutes at a temperature of 80 °C.

Table 1 summarizes the constituents and composition of the pure and modified TFC membrane films, while Figure 3 shows the polyamide layer formed between TMC and PIP.

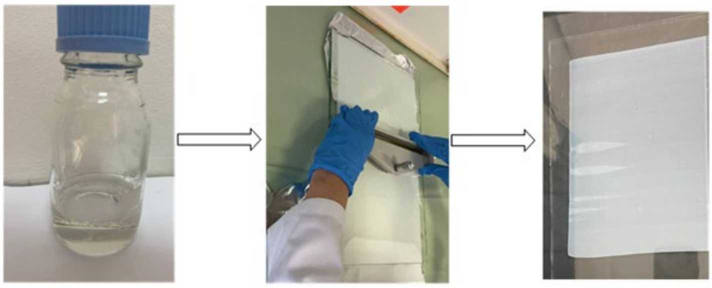

Figure 1: Preparation of support membrane

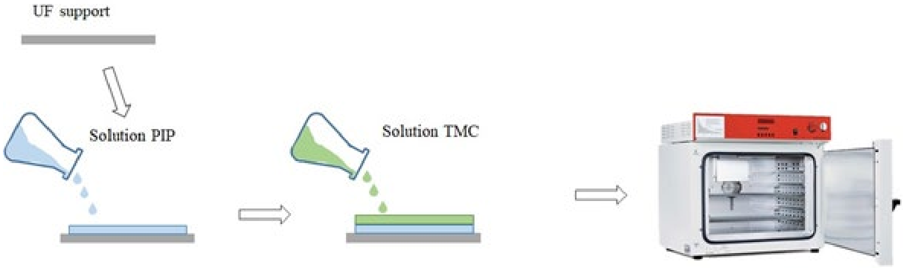

Figure 2: Membrane preparation steps TFC

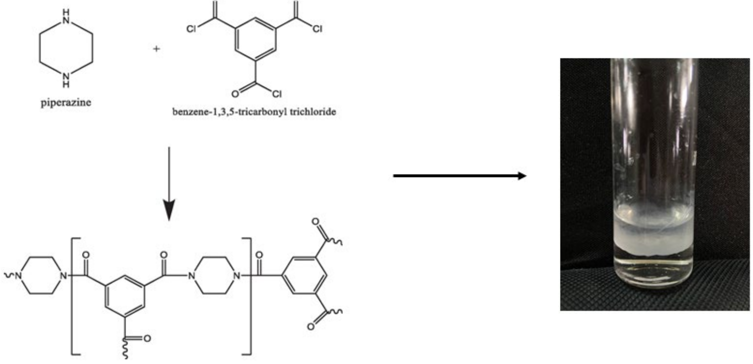

Figure 3: Interfacial polymerization reaction between PIP and TMC in TFC membrane

Table 1
Constituents and composition of the membranes

Membranes	AC	PAN	PES	PIP	TMC	CMCNa	Observation
TFC AC A1	18%	/	/	2%	0.7%	/	
TFC AC A2	18%	/	/	2%	0.7%	2%	Added the CMC-Na solution after IP
TFC AC A3	18%	/	/	2%	0.7%	2%	Added the CMC-Na solution before IP
TFC PAN B1	/	13%	/	2%	0.7%	/	
TFC PAN B2	/	13%	/	2%	0.7%	2%	Added the CMC-Na solution after IP
TFC PAN B3	/	13%	/	2%	0.7%	2%	Added the CMC-Na solution before IP
TFC PES C1	/	/	18%	2%	0.7%	/	
TFC PES C2	/	/	18%	2%	0.7%	2%	Added the CMC-Na solution after IP
TFC PES C3	/	/	18%	2%	0.7%	2%	Added the CMC-Na solution before IP

Characterization

The chemical structure and composition of the membrane surface were determined using ATR-FTIR (Frontier, Perkin Elmer) in the range of 4000–500 cm^{-1}, with a resolution of 0.5 cm^{-1}. The hydrophilicity of the TFC membrane surfaces was assessed by measuring the water uptake to evaluate their hydrophilic/hydrophobic properties. To determine the wet membrane weight, the membrane films were soaked in water for 24 hours, then dried with paper and weighed. Afterward, the membranes were dried in an oven at 80 °C for another 24 hours and weighed again to obtain the dry film weight.[18]

The water absorption was calculated using the following formula:

$$\text{Water absorption (\%)} = \frac{\text{MW}}{\text{Md}} \text{x}100 \quad (1)$$

where M_W – weight of the wet membrane, M_d – weight of the dry membrane.

Permeation test

Each membrane developed in this study was placed in a cross-flux test system, as outlined in our previous work.[18] To measure water flux and salt rejection, tests were conducted using a synthetic feed solution consisting of 7 g/L NaCl and 300 g/L $MgSO_4$ and $CaCO_3$, as well as a real seawater solution. The filtration cell had a surface area of 28.4 cm^2, and the transmembrane pressure varied from 10 to 30 bars at room temperature. The water flux was calculated based on the accumulated volume of permeated water over time. The following equations were used to determine water flux (J_h, L/m^2·h), permeability (L_p, L/m^2·h·bar), and rejection (T_r, %) for NaCl, $MgSO_4$, and $CaCO_3$:[19]

$$J_w = \frac{\Delta V}{\text{Am}\Delta t} \quad (2)$$

$$Lp = \frac{J}{\Delta P} \quad (3)$$

$$TR = \left(1 - \frac{C_p}{C_A}\right) x100 \quad (4)$$

where ΔV is the volume change of permeate water (L), Am is the membrane effective area (m^2), Δt is the testing time of filtration (h), and ΔP (bar) is the transmembrane pressure. C_A and Cp are the NaCl/$MgSO_4$/$CaCO_3$ concentrations (M) in feed and permeate solutions, respectively.

RESULTS AND DISCUSSION

Chemical structure

Examination of the FTIR spectrum of the pure cellulose acetate membrane illustrated in Figure 4 reveals the presence of several peaks, the most important of which are situated at 1035 cm^{-1}, 1230 cm^{-1}, and 1433 cm^{-1}. These peaks are attributed respectively to the C–O groups of the alcohol, the ester, and the CH_2 bonds.[20] These bands are identified in all TFC-CA composite membranes, widening and shifting towards higher wavenumbers with the incorporation of CMC-Na, implying the presence of stretching vibrations of the C=O groups of primary and secondary aliphatic alcohols in CMC-Na cellulose.[21]

The most significant absorption peaks in pure cellulose acetate membranes are located in the range of 1600–1800 cm^{-1}, with a prominent band fixed at 1739 cm^{-1}.[18] This peak is attributed to the vibration of the C=O bond of the acetate ester (–COCH3) in the side chain of cellulose acetate. It is worth noting that an enlargement or presence of such a peak at a similar value can be justified and identified by the presence of the C=O carbonyl function of the COO– group of the CMC-Na molecule incorporated in the final layer of the composite membrane. The interfacial polymerization induced by the reaction between PIP and TMC involves the formation of an amide bond on the selective layer of the TFC membrane. The specific peaks characterizing this bond are two: the first is located around 1651 cm^{-1} and is attributed to the C=O stretching vibrations of the –CO–NH groups, while the second is located around 1432 cm^{-1}, linked to the O–H stretching vibration of the carboxylic groups, which could be generated by the hydrolysis of TMC acyl chloride.[22] Due to the similarity of these peaks to those of the functional groups existing on the membrane films, they overlap with each other (those of cellulose acetate and CMC), making their detection difficult.

In the region of 3600–3050 cm^{-1}, the presence of a band located around 3484 cm^{-1} indicates the overlap of two vibration bands in pure cellulose acetate. The first is attributed to the OH group linked with C=O groups by hydrogen bonding, while the second corresponds to the free O–H group. A peak of moderate intensity is recorded at 2924 cm^{-1}, resulting from the stretching band of the existing methylene groups (–CH_2–). The incorporation of CMC-Na into the TFC AC C2 and C3 membranes implies the broadening of these peaks due to the increase in the density of OH groups within the membrane structure.

Figure 5 shows the ATR-FTIR spectra of pure and modified TFC PAN membranes. In the region of 1600–400 cm^{-1}, obvious peaks were detected at 1065 cm^{-1}, 1190 cm^{-1}, 1250 cm^{-1}, and 1360 cm^{-1}, corresponding to C–H, C=N stretching, and some stretching vibrations of functional groups such as –COO, C–OH, and C–O–C. The presence of the C–N stretching vibration at 1450 cm^{-1} demonstrates the presence of nitrogen on the film surface.[23]

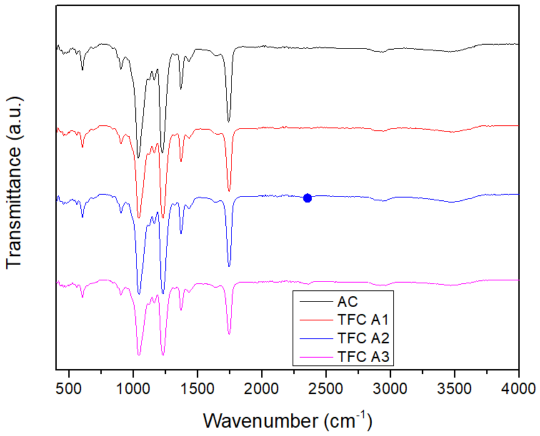

Figure 4: ATR-FTIR spectra of pure and modified TFC AC membranes

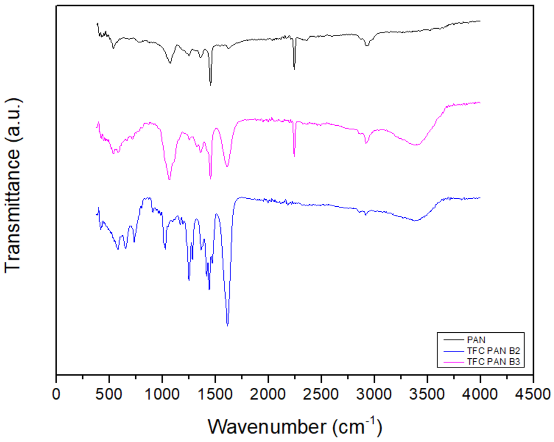

Figure 5: ATR-FTIR spectra of pure and modified TFC PAN membranes

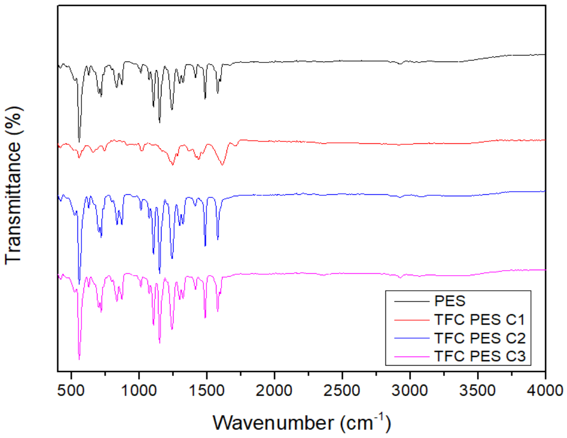

Figure 6: ATR-FTIR spectra of pure and modified TFC PES membranes

The absence of the bands located around 1608 cm^{-1} and 1415 cm^{-1} in the spectra of the PAN and TFC PAN membranes confirms that they correspond to groups linked to the CMC-Na molecule. These bands are attributed to vibrations related to carboxylates (–COO^-). These results confirm the successful coating of the CMC layer on the support. The vibration of the carbonyl group in CMC appears at lower wavenumbers because the COO^- group in CMC is more easily dissociated. The dissociation of protons in the carboxylic acid groups may cause electronic resonance in the carboxylic anions, resulting in a lower electron density in the carbonyl group. The wavenumber of the carbonyl group obtained from this study is closer to the value reported (1589 cm^{-1}) by Eliza *et al.* who used the same reagent. At the same time, these bands are very broad, which may obscure the presence of amide groups linked to the amide bond formed during the interfacial polymerization between PIP and TMC.[24]

In general, the formation of amide groups through interfacial polymerization is indicated by the presence of amide bands around 1660 cm^{-1} and 1480 cm^{-1}. However, the confirmation of these bands[25] based on the spectra cannot be definitively made, as they are superimposed on the bands of the functional groups present in the membrane constituents.

The stretching band of the C≡N group is observed around 2244 cm^{-1} and is detected in all polyacrylonitrile-based membranes. In the region of 3600–3050 cm^{-1}, the spectrum reveals the merged stretching vibration bands of O–H and N–H functional groups, with bands observed near 3400 cm^{-1}.[23] This band widens for the TFC PAN B2 and TFC PAN B3 membranes, attributed to the presence of the O–H group from the carboxylic group in the CMC-Na molecule. Additional bands are observed around 2830 and 2950 cm^{-1}, characterizing the stretching vibrations of the C–H bonds.

The FTIR spectrum of the PES polymer, shown in Figure 6, predominantly displays several absorption bands characteristic of the stretching vibrations and deformations of the functional groups in this polymer.[24] Notably, a band corresponding to the angular deformation of the SO_2 groups is located at 1300 cm^{-1}, a second band around 1241 cm^{-1} is characteristic of the ether function (C–O–C), and a band located around 1147 cm^{-1} characterizes the stretching vibration of the S=O bond.

Two bands located around 1485 cm^{-1} and 1578 cm^{-1}, characteristic of the stretching vibrations of the C=C bond in the benzene ring, were observed. In the composite membranes, the band at 1578 cm^{-1} broadens, confirming the presence of the main vibrational bands linked to asymmetric and symmetrical carboxylates (–COO^{-}) existing in the CMC-Na molecule.[25-26] A band at 3592 cm^{-1}, characteristic of the stretching vibration of the O–H bond, was observed with low intensity in the TFC PES membranes coated with the modified CMC-Na solution. This is due to the protonation of sodium carboxylate groups (–COONa) in CMC-Na during the cross-linking reaction with hydrochloric acid, resulting in the formation of –COOH groups. These results confirm the successful coating of the CMC layer on the PES support.

In conclusion, the FTIR study allowed the identification of all the functional groups present on the selective layer of both the pure and composite membranes. Regarding the amide bond, the bands attributed to it are identified in the range of 1400–1650 cm^{-1}. The presence of several similar peaks in this region complicates the definitive detection of this bond, confirming the successful completion of the interfacial polymerization of PI. According to this study, it was confirmed that the defining band of the carbonyl group (–COO^{-}) of the CMC-Na molecule is located at lower wavenumbers, leading to the appearance of its peak at lower values.

Membrane performance

According to the first graph (a) illustrated in Figure 7, where the pressure is set at 10 bars, the flux of all membranes remains nearly constant. The TFC membranes possessing AC cellulose acetate as a support exhibit the lowest flux, measuring approximately 24.2 L/m².h for the TFC AC A1 membrane. Conversely, the flux shows a significant increase upon the introduction of the molecule (CMC-Na) both before and after interfacial polymerization, with respective values of 52.61 and 57.87 L/m².h for the TFC AC A2 and TFC AC A3 membranes. These values demonstrate a twofold increase, indicating that the incorporation of the carboxymethyl acetate group from cellulose enhances the solution transfer, attributable to its hydrophilic properties.

Regarding the membranes based on TFC-PAN polyacrylonitrile, the pure TFC PAN B1 and TFC PAN B2 (PIP/TMC/CMC-Na) membranes present nearly constant flux values around 178 L/m².h. The highest flux observed was approximately 500 L/m².h for the TFC PAN B3 membrane (CMC-Na/PIP/TMC). It can be concluded that the incorporation of carboxymethyl cellulose prior to interfacial polymerization enhances permeability to pure water. Furthermore, the additional presence of the CMC layer on the surface of the highly porous PAN support reduces the resistance encountered by water molecules passing through the membrane, resulting in a significant increase in membrane flux for the TFC PAN B3 membrane. Figure 8 illustrates the flux of pure water as a function of transmembrane pressure. It was observed that the flux increases progressively with the rise in pressure. The resulting plot corresponds to a linear relationship, consistent with Darcy's law.

Indeed, the increase in transmembrane pressure enhances the driving force for the penetration of pure water through the membranes.[27] It was observed that the flux through the TFC AC A1 membrane is the lowest regardless of the applied pressure, reaching a minimum value of 25.25 L/m².h under a pressure of 10 bars and increasing to 168.5 L/m².h at a pressure of 25 bars, representing a sevenfold increase. These results corroborate literature data, indicating that pure cellulose acetate membranes exhibit low flux due to the nanometric nature of their pores, necessitating high pressure due to the compact morphology of their surface.

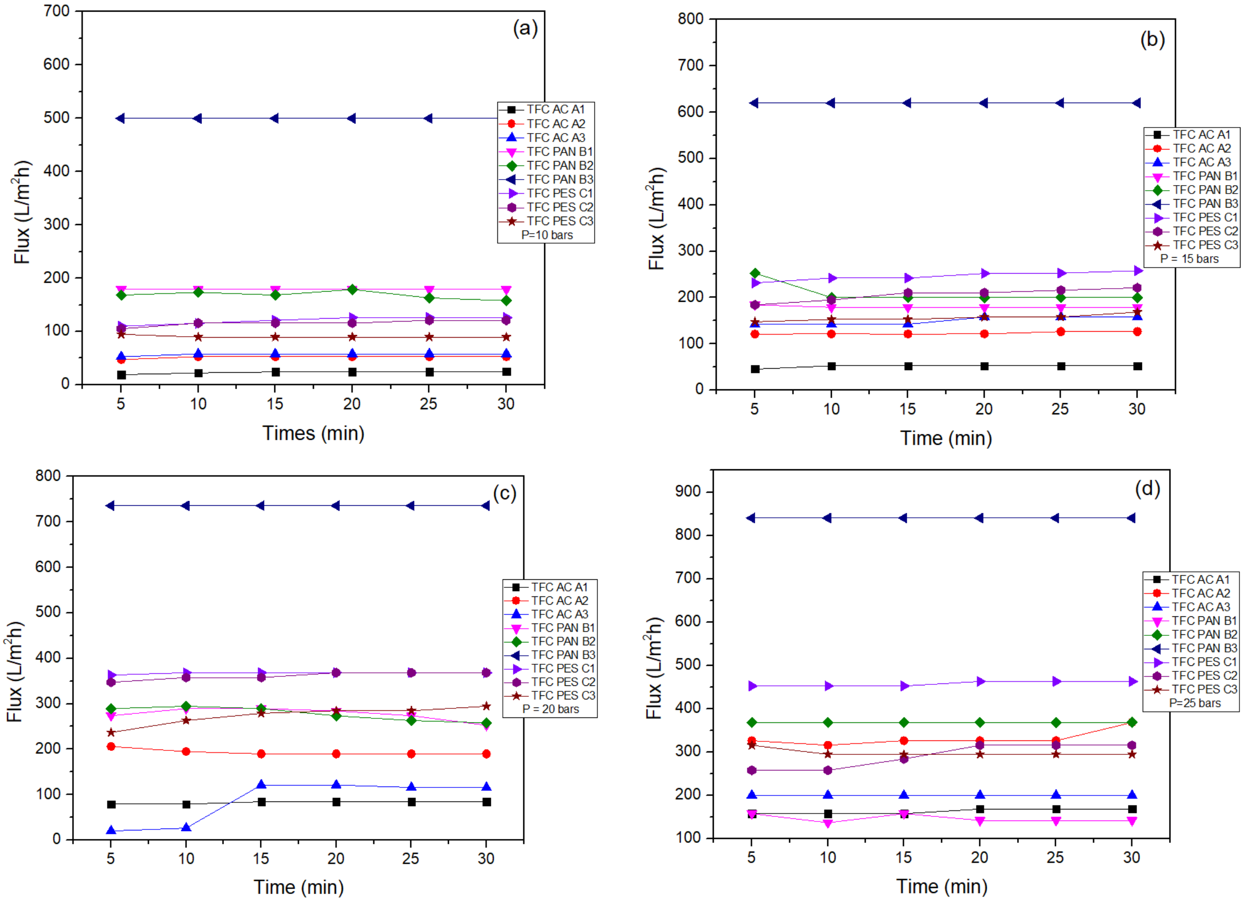

Figure 7: Variation of pure water flux as a function of time for all membranes at different pressure

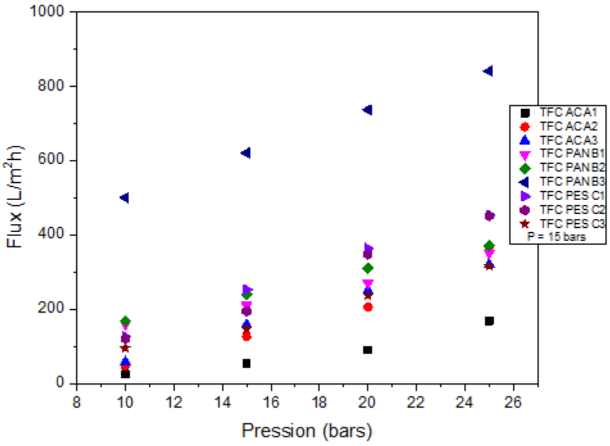

Figure 8: Flux variation as a function of transmembrane pressure

Table 2
Measurement of permeability for all the membranes developed

Membrane	TFC AC A1	TFC AC A2	TFC AC A3	TFC PAN B1	TFC PAN B2	TFC PAN B3	TFC PES C1	TFC PES C2	TFC PES C3
Permeability (L/m^2.h.bar)	9.55	21.4	20	7.36	13.32	24	21.74	13	14.72

Simultaneously, the flux density remains consistent between 10 and 20 bars for both pure and modified TFC PAN and TFC PES membranes. The flux is twice as high for all TFC PAN membranes and triples for TFC PES membranes. For instance, the TFC PAN B3 membrane demonstrates a maximum flux of 500 L/m².h under a transmembrane pressure of 10 bars, which increases to approximately 840 L/m².h at 25 bars. For membranes based on TFC PES polyethersulfone, the flux of the TFC PES C1 membrane rises from 126.25 L/m².h at 10 bars to 452.25 L/m².h at 25 bars.

The application of the CMC-Na solution to the membranes creates an additional layer, resulting in the formation of thicker, denser TFC layer films. In this context, an increase in applied pressure facilitates the passage of the solution through the membrane layers more rapidly and easily, thereby increasing the permeate flux.

The permeability of a membrane is one of the most fundamental characteristics describing its performance. The determination of this characteristic is based on calculating the slope of the curve representing the relationship between the filtration flux rate (Jv) and the transmembrane pressure difference (ΔP), i.e., Jv = f(ΔP). Table 2 presents the permeability values for the various membranes. It has been established that membrane permeability is closely associated with flux. This relationship indicates that the more permeable a membrane is, the greater the flux of substances passing through it.

In this study, the TFC PAN B3 membrane exhibited the best water permeability, with a permeability coefficient of Lp = 24 L/m².h.bar. In contrast, the pure PAN and TFC AC membranes, specifically TFC PAN B1 and TFC AC A1, are characterized by low permeability, with recorded values of 7.36 and 9.55 L/m².h.bar, respectively. The pure PES TFC PES C1 membrane displays a significantly higher value, measured at Lp = 21.74 L/m².h.bar, compared to the modified TFC PES C2 and C3 membranes, which contain a 2% by weight solution of CMC-Na before and after interfacial polymerization.

It can be inferred that this CMC-Na coating increases the diffusion path. Shi *et al.*[28] observed a similar behavior with their membrane coatings, concluding that the length of the diffusion path affects transport: shorter paths facilitate faster and less tortuous movement. Furthermore, the membrane supported by polyethersulfone exhibits a hydrophobic structure, resulting in reduced adherence between its surface and the carboxymethyl cellulose coating. In contrast, membranes based on polyacrylonitrile and cellulose acetate, which possess hydrophilic characteristics and functional groups such as amine and hydroxycarboxylic acid, promote better contact with water molecules. This difference highlights the significant impact of the constituent materials on the permeability properties of the membranes. Finally, a comparison of the different combinations of membrane materials (AC/CMC-Na, PAN/CMC-Na, and PES/CMC-Na) reveals that the PAN/CMC-Na configuration offers superior performance in terms of permeability compared to the other combinations.

In summary, optimizing the composition of membranes through the incorporation of CMC-Na can lead to significant improvements in their filtration performance. This affirms previous research, which deduced that the addition of a hydrophilic or porogenic agent improves the PEP, and implies better hydraulic permeability and therefore low hydraulic resistance of the membrane.[29]

Study of synthetic salt water permeation

Figure 9 illustrates the evolution of the flux of treated synthetic salt water as a function of time at a constant pressure of 15 bars. The results indicate that the flux behavior observed during the filtration tests of the synthetic solution is similar to that of pure water, presenting constant values with minimal variation over time. The best performances in terms of flux are noted for the TFC PAN B2 and TFC PES C3 membranes, with respective values of 193.96 and 162.51 L/m².h. Conversely, the TFC AC A1 and TFC PAN B3 membranes exhibit the lowest fluxes, measuring

47.18 L/m²·h for TFC AC A1 and 73.39 L/m²·h for TFC PAN B3. It is noteworthy that these values are lower than those obtained with pure water, indicating a significant loss of flux density. This reduction is likely due to concentration polarization, which causes the accumulation of certain substances near the membrane, thereby limiting the filtration flux.[30]

Several studies have shown that the concentration polarization layer is sensitive to changes in operating conditions, such as reductions in transmembrane pressure or alterations in surface roughness. It is important to note that polyacrylonitrile-based membranes have the most pronounced surface roughness and the greatest loss of flux. According to various studies, surface roughness is one of the primary parameters affecting the antifouling properties of a membrane.

Synthetic salt retention

Figure 10 presents the various salt concentrations and their corresponding retention rates. A significant elimination of calcium (Ca^{2+}) and magnesium (Mg^{2+}) ions was observed across all membranes. The retention rates for calcium range from 79% to 92%, while those for magnesium range from 84% to 97%.

The descending order of magnesium elimination is as follows: TFC C3 > TFC C2 > TFC B3 > TFC B1 > TFC A3 > TFC A1 > TFC B2 > TFC A2 > TFC C1. Among the membranes studied, the TFC PES C3 membrane exhibited the highest magnesium (Mg^{2+}) retention rate at 97%, while the TFC PES C1 membrane recorded the best calcium (Ca^{2+}) retention rate of 92%. These results indicate that membranes with a polyethersulfone support demonstrate superior separation rates for di- and monovalent ions. Additionally, membranes coated with a carboxymethyl cellulose (CMC) layer prior to interfacial polymerization showed enhanced salt retention. The retention of NaCl salt varies between the TFC AC A1 membrane and the TFC PES C3 membrane, with minimum and maximum rates of 48% and 68%, respectively. Notably, the elimination of the monovalent salt NaCl is lower than that of the divalent salts $MgSO_4$ and $CaCO_3$. From this histogram, it is evident that the retention of divalent ions complies with the freshwater standards established by the WHO (World Health Organization).

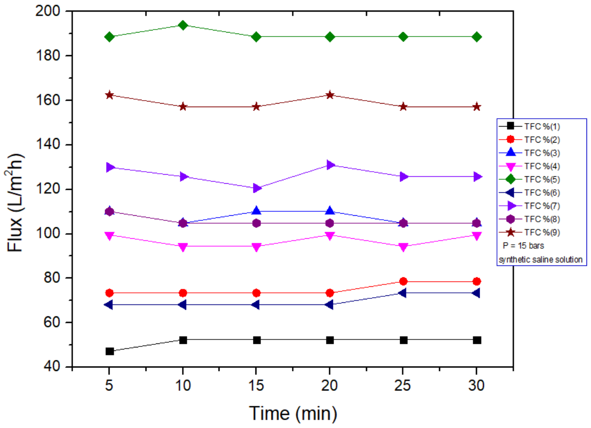

Figure 9: Variation of synthetic salt solution flux as a function of time for all membranes

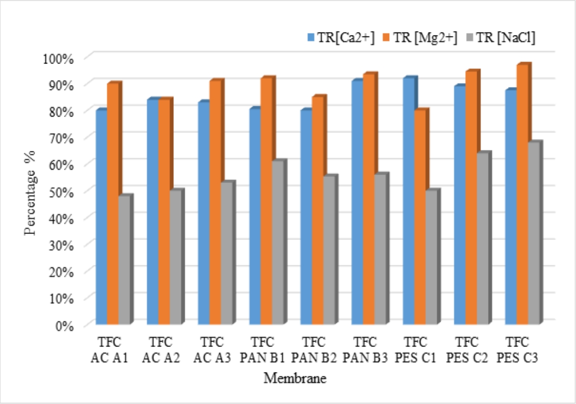

Figure 10: Salt retention rate for synthetic saline water

Table 3
Ionic radius, hydrated ionic radius and ion hydration energy

Ion	Ion ionic radius (nm)	Hydrated ionic radius (nm)	Hydration energy (kJ/mol)
Mg^{2+}	0.074	0.429	1921
Ca^{2+}	0.099	0.349	1584
Cl^{-}	0.181	0.347	515
SO_4^{2-}	0.230	0.380	1138

The rejection of inorganic salts by TFC membranes was observed in the following order: $MgSO_4 > CaCO_3 > NaCl$. A similar sequence was reported by Zhang *et al*.[30] and Sun *et al*.[31] in their evaluations of the desalination performance of modified polyamide NF membranes, where the order of release for inorganic salts was noted as $Na_2SO_4 > MgSO_4 > NaCl$. Both studies confirmed the presence of negative charges in the polyamide layer.

Generally, two main mechanisms can be considered for the separation performance of nanofiltration membranes: particle size screening and Donnan exclusion.[29] The observed order of salt rejection cannot be explained by a sieving mechanism, as the size of hydrated ions is significantly smaller than the pore size of the fabricated TFC-NF membranes (see Table 3). Donnan exclusion arises from electrostatic interactions between the surface charges of the membrane's active layer and the ions in solution. According to this theory, negatively charged NF membranes tend to repel multivalent anions (such as SO_4^{2-}) more than monovalent anions (such as Cl^-), while attracting multivalent cations (such as Mg^{2+}) more than monovalent cations (such as Na^+).[31-32] It is noteworthy that a negative charge was induced in the selective layer by coating CMC molecules onto the PES support. This negative charge can be attributed to the carboxylic groups of the CMC molecules, thus supporting the explanation of the observed order of salt rejection via the Donnan exclusion mechanism.[33-34]

In conclusion, the TFC PES C3 membrane, which contained a CMC coating prior to interfacial polymerization, demonstrated optimal performance in terms of selectivity, with a pure water flux of 162.51 $L/m^2 \cdot h$. This optimal membrane was capable of rejecting 97%, 79%, and 68% of $MgSO_4$, $CaCO_3$, and NaCl solutions, respectively, indicating a suitable desalination performance for the TFC-NF membrane fabricated under low pressure.

Study of seawater permeation

Figure 11 presents the variation of seawater flux as a function of time for all membranes tested. A decrease in flux was observed for the majority of TFC membranes. The highest flux was recorded for the TFC PES C3 membrane, achieving a value of 314.53 $L/m^2 \cdot h$ at a time of 30 minutes. The TFC PAN B3 membrane, based on polyacrylonitrile, showed the same flux behavior to that of synthetic saline water, recording the lowest flux at 246.38 $L/m^2 \bullet h$, which confirms previous observations regarding its surface roughness.

Moreover, the TFC AC A1 membrane consistently maintained the lowest flux. Generally, the reduction in flux with increasing salt content in the feed can be attributed to the rise in concentration polarization at the membrane surface as feed salinity increases. It was noted that the tested membranes retained a maximum of their initial fluxes, with the lowest flux loss observed for the TFC PES C membranes, which recorded losses of 9% and 10% for the TFC PES C1 membrane (without CMC) and TFC PES C2, respectively. This can be explained by the hydrophobic nature of polyethersulfone (PES), which mitigates the concentration of salts on its surface.

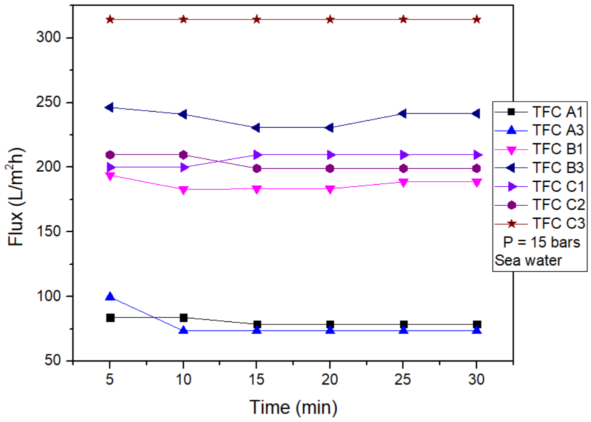

Figure 11: Variation of seawater flux as a function of time for all membranes

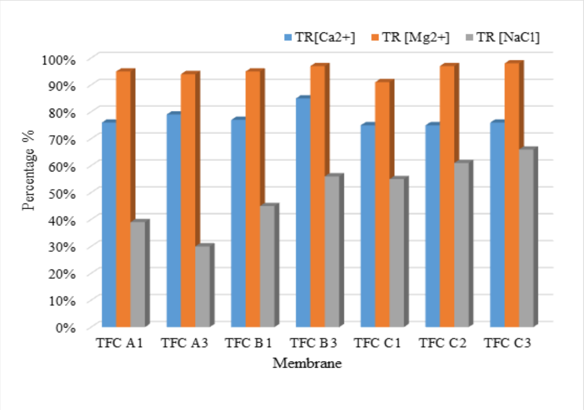

Figure 12: Salt retention rate for Tipaza sea water water

Study of $MgSO_4$, $CaCO_3$, and NaCl retention from seawater

The selective separation study aimed to evaluate the treatment of water from real sources, particularly seawater, characterized by a pH of 8, conductivity of 50 mS/cm, and salinity of 32 g/L. For this study, several membranes were selected and tested at a pressure of 15 bars. The primary objective was to analyze the effectiveness of these membranes in separating di- and monovalent salts from seawater. Figure 12 shows a satisfactory elimination of magnesium (Mg^{2+}) for all tested membranes, with retention rates ranging from 95% to 98%, and for calcium (Ca^{2+}), with values between 75% and 85%. Among the different membranes studied, the TFC PES membranes exhibited the best salt retention, and the incorporation of the CMC molecule prior to interfacial polymerization enhanced the salt retention rate, thus confirming results from brackish water studies.

The TFC PES C3 membrane particularly excelled in its high retention rates for magnesium (Mg^{2+}), calcium (Ca^{2+}), and salt (NaCl), achieving rates of 98%, 76%, and 66%, respectively. This performance confirms previous results and affirms that optimal retention is achieved for the TFC membrane based on PES polyethersulfone with the CMC coating before interfacial polymerization, affirming previous research, which proved that PES UF support membranes can be modified by applying a thin layer of hydrophilic polymer and can be used in desalination.[35-39] Comparing these results with those obtained for ions reconstituted in the laboratory (synthetic waters) reflects different values. This difference is entirely logical if the influence of the ions on the retention rate is taken into account.

In summary, the studies of salt elimination across different membranes allow us to conclude that, in terms of selectivity, the retention of di- and monovalent salts is highest for the TFC PES C3 membrane, which exhibits a flux of 314.53 L/m².h. The TFC PAN B3 membrane can be considered effective in retaining divalent salts, with a flux of 230.66 L/m²·h. However, the retention of monovalent salts remains insufficient to meet the salinity standards set by the WHO. The salt rejection rates of the membranes studied lead to the following decreasing order: TFC PES C3 > TFC PES B3 > TFC PAN C2 > TFC PAN B1 > TFC PES C1 > TFC AC A1 > TFC AC A3.

In conclusion, the salt rejection rates for the membranes follow this sequence: $MgSO_4 > CaCO_3 > NaCl$. The TFC PES C3 and TFC PAN B3 membranes are considered the most reliable and effective for the elimination of divalent salts from a flux perspective. Nevertheless, the TFC PES C3 membrane demonstrates optimal parameters, achieving a flux of 314 L/m².h at 20 bars, with retention rates of 98% for Mg^{2+}, 76% for Ca^{2+}, and 66% for NaCl, all of which align with WHO standards for divalent ions. Such membranes are indeed useful for reducing water hardness and for the partial desalination of brackish water. These results affirm that the retention of monovalent salts is constrained by the nanofiltration process.

CONCLUSION

This study aimed to achieve several objectives. The first was to develop new thin-film composite (TFC) membranes by introducing an additional layer of a hydrophilic compound to enhance their efficiency in terms of flux and permeability. The second objective involved utilizing different types of polymeric materials for the fabrication of the lower layer of the TFC membrane, allowing for a comparative analysis of their influence on the membrane's morphology and efficiency. The final goal was to validate the membranes' performance regarding flux and rejection rates, while maintaining optimal flux and improving selectivity. TFC membranes were successfully prepared via interfacial polymerization on CA, PAN and PES supports, each with a thickness of 250 µm. An ultra-thin active layer composed of PA was formed through the condensation of PIP and TMC. A solution of CMC-Na was introduced before and after the interfacial polymerization reaction to enhance the membrane's hydrophilicity, performance, and properties.

FTIR analyses confirmed the presence of characteristic bands associated with the functional groups of the various components in all produced membranes.

In terms of material transfer, coating the membranes with a CMC-Na layer improved the flux, permeability, and water adsorption for the modified TFC AC and PAN membranes, both before and after interfacial polymerization. The TFC PAN B3 membrane demonstrated optimal flux and permeability values of 500 L/m².h and 24 L/m².h.bar, respectively. Likewise, the flux doubled for the modified TFC AC membranes. On the other hand, the modification of the TFC PES membranes demonstrated an opposite character, the CMC-Na layer increased the water diffusion path, resulting in reduced permeation parameters.

The performance of the developed membranes was evaluated in terms of rejection rates. All modified membranes presented very satisfactory retention rates for divalent salts. Among them, the TFC PES C3 membrane emerged as the most reliable and effective in terms of selectivity, achieving retention rates of 98% for Mg^{2+}, 76% for Ca^{2+}, and 66% for NaCl. Thus, the incorporation of CMC into the TFC structure enhanced the efficiency of the TFC PES C3 membrane regarding salt rejection.

The developed membranes are classified as nanofiltration membranes, successfully removing divalent salts, although the retention of monovalent salts remains partial.

REFERENCES

[1] S. S. Salih, A. Mahdi, M. Kadhom and T. K. Ghosh, *J. Environ. Chem. Eng.*, **7**, 103407 (2019), https://doi.org/10.1016/j.jece.2019.103407

[2] A. Diaf, H. Aburideh and F. K. Benabdelaziz, *J. Renew. Energ.*, **19**, 69 (2023), https://doi.org/10.54966/jreen.v19i1.549

[3] S. Hout, Z. Salem, D. Tassalit, Z. Tigrine, H. Aburideh *et al.*, *Water Environ. J.*, **35**, 473 (2020), https://doi.org/10.1111/wej.12644

[4] M. Kadhom, M. Al-Furaiji, S. Salih, M. A. Al-Obaidi, G. H. Abdullah *et al.*, *J. Water Process Eng.*, **51**, 103402 (2023), https://doi.org/10.1016/j.jwpe.2022.103402

[5] M. Al-Furaiji, K. R. Kalash, M. A. Kadhom and Q. F. Alsalhy, *Desalin. Water Treat.*, **215**, 50 (2021), https:/doi.org/10.5004/dwt.2021.26764

[6] P. P. Li, S. M. Xue, U. Shareef, Z. L. Xu and C. H. Ji, *J. Membr. Sci.*, **624**, 119104 (2021), https://doi.org/10.1016/j.memsci.2021.119104

[7] D. Zioui, H. Salazar, L. Aoudjit, P. M. Martins and S. L. Méndez, *Polymers*, **12**, 42 (2020), https://doi.org/10.3390/polym12010042

[8] P. P. Li, U. Shareef, Z. L. Xu, D. Taymazov, Y. Z. Wu *et al.*, *J. Membr. Sci.*, **641**, 119937 (2022), https://doi.org/10.1016/jmemsci.2021.119937

[9] M. Kadhom, *Chem. Eng. Res. Des.*, **191**, 472 (2023), https://doi.org/10.1016/j.cherd.2023.02.002

[10] A. K. Ajpai, S. K. Shukla, S. Bhanu and S. Kankane, *Progress Polym. Sci.*, **33**, 1088 (2008), https://doi.org/10.1016/j.progpolymsci.2008.07.005

[11] S. Khan, A. K. Ghosh, V. Ramachandhran, J. Bellare, M. S. Hanra *et al.*, *Desalination*, **128**, 57 (2000), https://doi.org/10.1016/S0011-9164(00)00023-0

[12] G. Jonsson and C. E. Boesen, *Desalination*, **17**, 145 (1975), https://doi.org/10.1016/S0011-9164(00) 84054-0

[13] J. C. Su, Q. Yang, J. F. Teo and T. S. Chung, *J. Membr. Sci.*, **355**, 36 (2010), https://doi.org/10.1016/j.memsci.2010.03.003

[14] J. Deng, Q. He, Z. Wu and W. Yang, *J. Polym. Sci. Part A*: *Polym. Chem.*, **46**, 2193 (2008), https://doi.org/10.1002/pola.22554

[15] K. Guo and C. C. Chu, *J. Polym. Sci. Part A*: *Polym. Chem.*, **43**, 3932 (2005), https://doi.org/10.1002/pola.20463

[16] H. Aburideh, N. Kasbadji, M. W. Naceur, Z. Tigrine, D. Tassalit *et al.*, *Cellulose Chem. Technol.*, **53**, 583 (2019), https://doi.org/10.35812/CelluloseChemTechnol.2019.53.58

[17] I. Karbownik, M. Fiedotb, O. Rac, P. S. Wozniak, T. Rybicki *et al.*, *Polymer*, **75**, 97 (2015), https://doi.org/10.1016/j.polymer.2015.08.015

[18] H. Aburideh, Z. Tigrine, D. Zioui, S. Hout, D. Tassalit *et al.*, *Cellulose Chem. Technol.*, **55**, 679 (2021), https://doi.org/10.35812/CelluloseChemTechnol.2021.55.59

[19] S. Paralikar, J. Simonsen and J. Lombardi, *J. Membr. Sci.*, **320**, 248 (2008), https://doi.org/10.1016/j.memsci2008.04.009

[20] M. K. M. Haafiz, S. J. Eichhorn, A. Hassan and M. Jawaid, *Carbohyd. Polym.*, **93**, 628 (2013), https://doi.org/10.1016/j.carbpol.2013.01.035

[21] S. Yuwono, E. Wahyuningsih, N. Oviany, A. Kiswandono, W. Simanjuntak *et al.*, *Mater. Plast.*, **57**, 225 (2020), https://doi.org/10.37358/MP.20.4.5422

[22] L. Chiem, L. Huynh, J. Ralston and D. A. Beattie, *Langmuir*, **24**, 8036 (2008), https://doi.org/10.1021/la800490t

[23] I. Karbownik, M. Fiedot, O. Rac, P. Wozniakb, T. Rybicki *et al.*, *Polymer*, **75**, 97 (2015), http://dx.doi.org/10.1016/j.polymer.2015.08.015

[24] M. Y. Eliza, M. Shahruddin, J. Noormaziah and W. Chung, *J. Med. Biol. Eng.*, **4**, 165 (2015), https://doi.org/10.12720/jomb.4.2.165-169

[25] R. J. Petersen, *J. Membr. Sci.*, **83**, 81 (1993), https://doi.org/10.1016/0376-7388(93)80014-O

[26] S. Chou, R. Wang, L. Shi, Q. She, C. Tang *et al.*, *J. Membr. Sci.*, **389**, 25 (2012), https://doi.org/10.1016/j.memsci.2011.10.002

[27] V. Pereira, A. M. Isloor, U. K. Bhat, A. F. Ismail, A. Obaid *et al.*, *RSC Adv.*, **5**, 53874 (2015), https://doi.org/10.1039/C5RA07994B

[28] Y. Shi, J. Huang, G. Zeng, W. Cheng, H. Yu *et al.*, *J. Colloid Interface Sci.*, **531**, 433 (2018), https://doi.org/10.1016/j.jcis.2018.07.079

[29] J. G. Ivas, M. I. Miranda, M. I. Clar, J. A. M. Roca and L. P. Alcaniz, *Separ. Purif. Technol.*, **128**, 45 (2014), https://dx.doi.org/10.1016/j.sppur.2014.03.012

[30] H. Aburideh, Z. Tigrine, L. Aoudjit, Z. Belgroun, K. Redjimi *et al.*, *Cellulose Chem. Technol.*, **55**, 1153 (2021), https://doi.org/10.35812/CelluloseChemTechnol.2021.55.99

[31] Z. Zhang, G. Kang, H. Yu, Y. Jin and Y. Cao, *J. Membr. Sci.*, **570**, 403 (2019), https://doi.org/10.1016/j.memsci.2018.10.061

[32] Z. Sun, Q. Wu, C. Ye, W. Wang, L. Zheng *et al*., *Nano Lett*., **19**, 2953 (2019), https://doi.org/10.1021/acs.nanolett.9b00060

[33] D. Zioui, L. Aoudjit, H. Aburideh and Z. Tigrine, *Cellulose Chem. Technol*., **56**, 353 (2022), https://doi.org/10.35812/cellulosechemtechnol.2022.56.31

[34] D. Zioui, L. Aoudjit, F. Touahra and K. Bachari, *Cellulose Chem. Technol*., **56**, 1101 (2022), https://doi.org/10.35812/CelluloseChemTechnol.2022.56.98

[35] L. F. Fang, M. Y. Zhou, L. Cheng, B. K. Zhu, H. Matsuyama *et al*., *J. Membr. Sci*., **572**, 28 (2019), https://doi.org/10.1016/j.memsci.2018.10.054

[36] M. Rahbari-Sisakht, A. F. Ismail and T. Matsuura, *Sep. Purif. Technol*., **88**, 99 (2012), https://doi.org/10.1016/j.seppur.2011.12.012

[37] A. K. Ghosh and E. M. V. Hoek, *J. Membr. Sci*., **336**, 140 (2009), https://doi.org/10.1016/j.memsci.2009.03.024

[38] K. Y. Wang, T.-S. Chung and J.-J. Qin, *J. Membr. Sci*., **300**, 6 (2007), https://doi.org/10.1016/j.memsci.2007.05.035

[39] L. Li, J. Dong and T. M. Nenoff, *Sep. Purif. Technol*., **53**, 42 (2007), https://doi.org/10.1016/j.seppur.2006.06.012